Bioorganic & Medicinal Chemistry 18 (2010) 6044–6054

Contents lists available at ScienceDirect

Bioorganic & Medicinal Chemistry

journal homepage: www.elsevier.com/locate/bmc

Syntheses and pharmacological characterization of novel thiazole derivatives as potential mGluR5 PET ligands

Cindy A. Baumann, Linjing Mu, Nicole Wertli, Stefanie D. Krämer, Michael Honer, Pius A. Schubiger, Simon M. Ametamey *

Center for Radiopharmaceutical Sciences, ETH Zurich (Swiss Federal Institute of Technology), Wolfgang-Pauli Strasse 10, 8093 Zurich, Switzerland

ARTICLE INFO

Article history:
Received 18 January 2010
Revised 8 June 2010
Accepted 20 June 2010
Available online 25 June 2010

Keywords:
Metabotropic glutamate receptor subtype 5 (mGluR5)
PET imaging
Fluorine-18
Neurological disorders

ABSTRACT

Four novel thiazole containing ABP688 derivatives were synthesized and evaluated for their binding affinity towards the metabotropic glutamate receptor subtype 5 (mGluR5). (*E*)-3-((2-(Fluoromethyl)thiazol-4-yl)ethynyl)cyclohex-2-enone *O*-methyl oxime (FTECMO), the ligand with the highest binding affinity (K_i = 5.5 ± 1.1 nM), was labeled with fluorine-18. [^{18}F]-FTECMO displayed optimal lipophilicity (log $D_{pH7.4}$ = 1.6 ± 0.2) and high stability in rat and human plasma as well as sufficient stability in rat liver microsomes. In vitro autoradiography with [^{18}F]-FTECMO revealed a heterogeneous and displaceable binding in mGluR5-rich brain regions. PET imaging with [^{18}F]-FTECMO in Wistar rats, however, showed low brain uptake. Uptake of radioactivity into the skull was observed suggesting in vivo defluorination. Thus, although [^{18}F]-FTECMO is an excellent ligand for the detection of mGluR5 in vitro, its in vivo characteristics are not optimal for the imaging of mGluR5 in rats in vivo.

1. Introduction

Glutamate is the predominant excitatory neurotransmitter in the mammalian central nervous system (CNS). Glutamate receptors form a large family, which can be classified into ionotropic and metabotropic glutamate receptors. The ligand-gated, cation-selective ion channels that form the ionotropic glutamate receptors (iGluRs) mediate fast excitatory neurotransmission. IGluRs include kainate, α-amino-3-hydroxy-5-methyl-4-isoxazolepropionic acid (AMPA) and *N*-methyl-D-aspartate (NMDA) receptors. Metabotropic glutamate receptors (mGluRs) are known to be involved in the modulation of iGluRs and appear to fine-tune neuronal activity. The subclass of mGluRs consists of eight G-protein coupled receptors (GPCRs) that are sub-divided according to their receptor pharmacology, amino acid sequences and their secondary messenger systems into three groups (groups I–III). Group I comprises mGluR1 and mGluR5 that are mainly post-synaptic receptors activating G_q proteins and phospholipase C as a secondary messenger. Group II consists of mGluR2 and mGluR3 while mGluR4, mGluR6, mGluR7, and mGluR8 form group III. Receptors of both groups use a G_i protein for signal transduction.[1,2]

MGluRs have been implicated in numerous CNS disorders. Notably, mGluR5, which is predominantly located in the hippocampus, striatum, and cortex,[3] was shown to be involved in neurodegenerative diseases such as Alzheimer's disease,[4,5] Parkinson's disease[6,7] or other disorders such as depression,[8] anxiety,[9] schizophrenia,[10,11] neuropathic pain,[12,13] drug addiction,[14] and fragile X syndrome.[15] However, the function of mGluR5 is not yet well understood and it is generally agreed that a better understanding of the physiological and pathophysiological roles of the receptor will open new avenues for the development of diagnostic tools and effective drugs for the above mentioned CNS disorders.[16]

Positron emission tomography (PET) is a non-invasive in vivo imaging technique that offers the possibility to visualize and analyze mGluR5 expression under various physiological and pathophysiological conditions. Our group reported the first successful in vivo imaging of mGluR5 in rodents and humans using carbon-11 labeled ABP688 (Fig. 1, **4**).[17] The short physical half-life of carbon-11 ($t_{1/2}$ = 20 min), however, does not permit the widespread use of [^{11}C]-ABP688. More advantageous seems the use of fluorine-18 ($t_{1/2}$ = 110 min) due to the possibility of satellite distribution of potential fluorine-18 labeled compounds to centers without a cyclotron facility. Recently, a number of fluorine-18 labeled compounds for imaging mGluR5 have been reported. Among these are [^{18}F]F-PEB[18,19] (Fig. 1, **1**) and the thiazole derivatives [^{18}F]F-MTEB[18] (Fig. 1, **2**) and [^{18}F]SP203[20] (Fig. 1, **3**). Microwave heating was applied for the radiosynthesis of [^{18}F]F-PEB and [^{18}F]F-MTEB but only low radiochemical yields were obtained. The low radiochemical yields were improved later on when thermal heating was employed.[21] [^{18}F]F-PEB[18,19] was recently used for the in vivo imaging of mGluR5 in human studies.[22] For [^{18}F]SP203 (Fig. 1, **3**), radiodefluorination was observed in PET studies involving monkeys. In humans, however, low uptake of

* Corresponding author.
E-mail address: simon.ametamey@pharma.ethz.ch (S.M. Ametamey).

0968-0896/$ - see front matter © 2010 Elsevier Ltd. All rights reserved.
doi:10.1016/j.bmc.2010.06.070

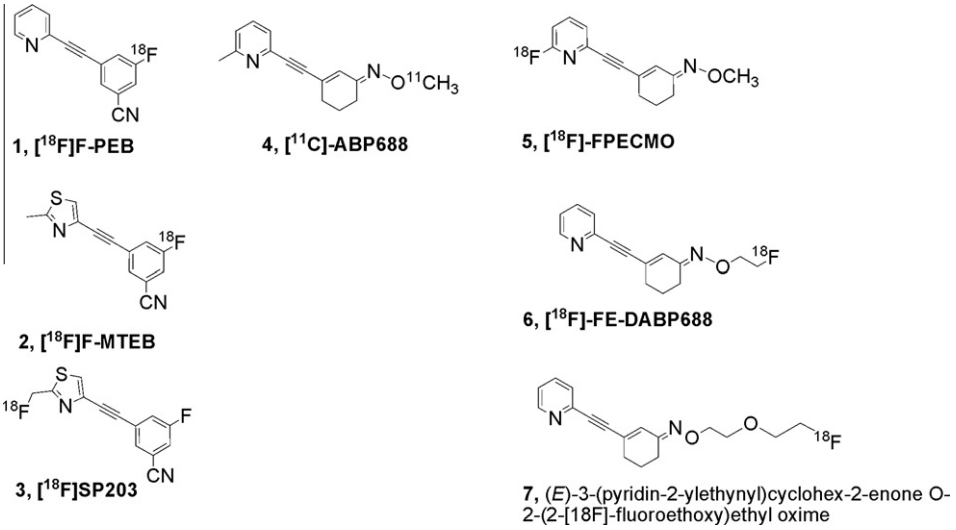

Figure 1. Structures of mGluR5 radioligands.

radioactivity into the skull was observed, suggesting a lower radiodefluorination rate in humans.[23] Recently, our group also reported on two novel fluorine-18 labeled analogues of ABP688: [^{18}F]-FPECMO[24] (Fig. 1, **5**) and [^{18}F]-FE-DABP688[25] (Fig. 1, **6**). While [^{18}F]-FPECMO underwent radiodefluorination in vivo in rats, [^{18}F]-FE-DABP688 displayed unfavorable pharmacokinetics. As part of our program to develop fluorine-18 labeled derivatives of ABP688, we designed four novel compounds based on the structural elements of the two most successful mGluR5 PET ligands, [^{11}C]-ABP688 and [^{18}F]SP203. Herein, we report the syntheses and binding affinities of the four novel thiazole containing ABP688 derivatives. Furthermore, we report on the radiolabeling, in vitro and in vivo evaluation of the most promising candidate, [^{18}F]-FTECMO.

2. Results

2.1. Chemistry

The syntheses of four novel mGluR5 ligands (**11**, **14**, **24**, and **25**) containing thiazole moieties were achieved in satisfactory overall yields, although none of the synthetic steps was optimized. Reference compound **11** was obtained via convergent synthesis (Scheme 1). First, compound **8** was converted into methyl oxime **9** in analogy to the method described for the preparation of intermediate **13**. Compound **10** was obtained according to the procedure previously described.[20] 2-(Fluoromethyl)-4-(ethynyl)thiazole in turn was obtained from **10** in situ by addition of TBAF to the Sonogashira reaction mixture. 2-(Fluoromethyl)-4-(ethynyl)thiazole was then coupled to the *trans*-isomer of **9** to afford end product **11** in 11% yield. In a similar manner, 2-bromothiazole (**12**) was coupled to starting material **13**,[24] which was prepared according to the procedure recently described,[26] to afford **14** in moderate yield (Scheme 2). The

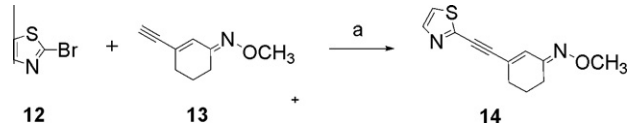

Scheme 2. Synthesis of model compound **14**. Reagents and conditions: (a) $Pd(PPh_3)_4$, CuI, Et_3N, DMF, rt, 48 h, 26%.

Sonogashira coupling of the *trans*-oxime **17**,[26] to either 2-methyl-4-bromothiazole or 4-bromothiazole gave acceptable yields of compounds **18** and **19**. Both intermediates were reacted with (2-(2-bromoethoxy)ethoxy)(*tert*-butyl)dimethylsilane to afford the TBS protected intermediates **20** and **21**, respectively. Compounds **20** and **21** were desilylated using TBAF and reacted with benzylsulfonylchloride to give tosylates **22** and **23**. Nucleophilic substitution reaction of the tosyl leaving group with dry TBAF afforded final products **24** and **25** (Scheme 3).

The precursor for the preparation of the radiolabeled analogue of compound **11** was synthesized in analogy to the method described for the synthesis of the precursor for [^{18}F]SP203.[20] Compound **26** was prepared according to the procedure reported by Siméon et al.[20] The Sonogashira coupling of compound **26** and intermediate **13** was accomplished in reasonable yields and gave compound **27**. Compound **27** was treated with TBAF to yield alcohol **28**. In the final step, alcohol **28** was converted to the bromide precursor **29** using CBr_4 and PPh_3 (Scheme 4).

2.2. In vitro binding assays

Compounds **11**, **14**, **24**, **25** (Table 1) were investigated for their binding affinity towards mGluR5. The four compounds exhibited binding affinities in the nanomolar range. The fluoromethyl-thiazole analogue, **11**, gave a K_i value of 5.5 ± 1.1 nM (Fig. 2), whereas

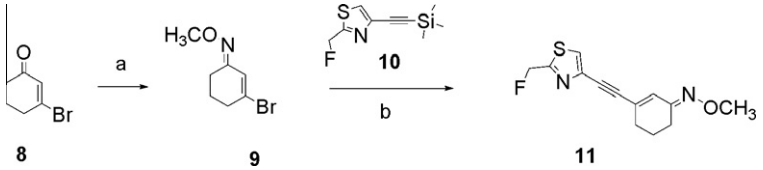

Scheme 1. Synthesis of FTECMO (**11**, (*E*)-3-((2-(fluoromethyl)thiazol-4-yl)ethynyl)cyclohex-2-enone *O*-methyl oxime). Reagents and conditions: (a) NH_2OCH_3·HCl, pyridine, rt, 18 h, 63%; (b) CuI, $Pd(PPh_3)_4$, DMF, Et_3N, TBAF, rt, 20 h, 11%.

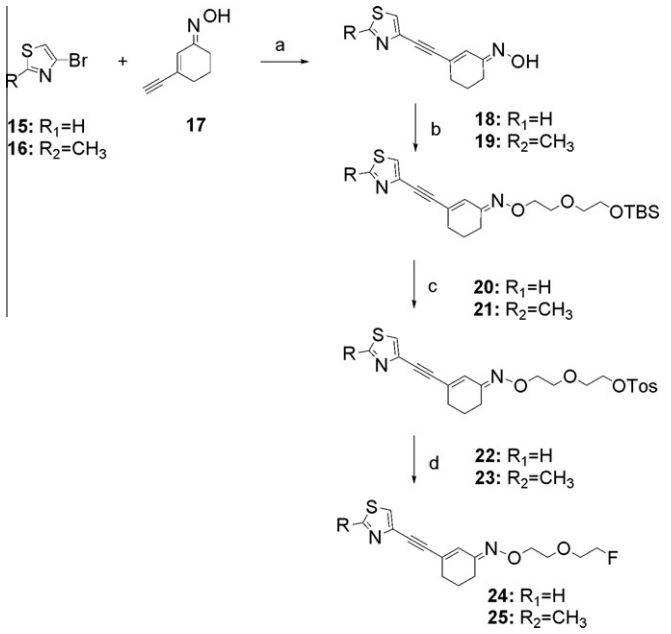

Scheme 3. Syntheses of two thiazole analogues (**24** and **25**) of the mGluR5 radioligand **7** (Fig. 1). Reagents and conditions: (a) DMF, $Pd(PPh_3)_4$, CuI, Et_3N, rt, 24 h, 24–54%; (b) DMF, NaH, (2-(2-bromoethoxy)ethoxy)(*tert*-butyl)dimethylsilane, rt, 2 h, 72–80%; (c) (1) THF, TBAF, rt, 1.5 h; (2) CH_2Cl_2, toluenesulfonylchloride, 0 °C, rt, 12 h, 85–91%; (d) THF, TBAF, 60 °C, 5 h, 25–28%.

the comparable 2-yl-thiazole analogue **14**, lacking a methyl group on the thiazole ring, exhibited a slightly reduced affinity with a K_i value of 20.3 ± 6.3 nM. Compounds **24** and **25** with ethoxy side chain substitutions at the oxime moiety exhibited lower binding affinities towards mGluR5. The desmethyl analogue **24** gave a K_i value of 36.0 ± 11.1 nM, while compound 25 showed a slightly higher affinity (K_i = 21.9 ± 7.0 nM) for mGluR5. Since compound **11** displayed the highest binding affinity of all the four candidates tested, it was selected for radiolabeling and further evaluation.

2.3. Radiosynthesis of [^{18}F]-FTECMO

A one-step radiolabeling procedure was successfully applied for the labeling of [^{18}F]-FTECMO with fluorine-18 (Scheme 5). The reaction proceeded well in MeCN at 90 °C in a reaction time of 10 min and the final product was obtained in a radiochemical yield of up to 45% (decay corrected). The total synthesis time (from end of bombardment) including the formulation of [^{18}F]-FTECMO was 60 min. Radiochemical purity was greater than 99% (Fig. 3) and the specific radioactivity ranged from 50 to 120 GBq/μmol (n = 6). The identity of the radioligand was confirmed by co-injection with reference compound **11**.

Table 1
Binding affinity of four thiazole derivatives **11**, **14**, **24** and **25** towards mGluR5

Ligand	Structure of the compounds	K_i (nM)
11	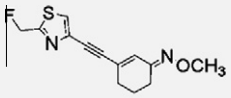	5.5 ± 1.1
14	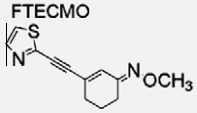	20.3 ± 6.3
24	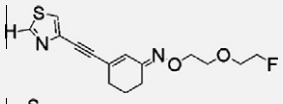	36.0 ± 11.1
25	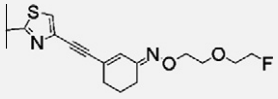	21.9 ± 7.0

2.4. Determination of log $D_{pH7.4}$

The lipophilicity of [^{18}F]-FTECMO was determined by the shake flask method at physiological pH in analogy to the method described by Wilson et al.[27] A log $D_{pH7.4}$ of 1.6 ± 0.2 was obtained for [^{18}F]-FTECMO and this value compares favorably to the calculated log P value of 1.9.

2.5. In vitro stability

Stability studies in rat and human plasma revealed no radioactive degradation products of [^{18}F]-FTECMO at 37 °C after an incubation period to 120 min. In rat liver microsomes, 93% of the parent compound was still intact after 60 min of incubation. One minor radioactive degradation product, more polar than the parent compound, was detected by HPLC.

2.6. In vitro autoradiography

Incubation of rat brain slices with [^{18}F]-FTECMO using two different concentrations (0.5 nM or 5 nM) resulted in a heterogeneous binding of the tracer with the highest accumulation in mGluR5-rich brain regions such as the hippocampus, striatum, and cortex (Fig. 4). As expected, accumulation of radioactivity in the cerebellum was negligible. Furthermore, blocking studies in which the rat brain slices were incubated with [^{18}F]-FTECMO together with an excess of unlabeled ABP688 (500 nM) led to substantially reduced and homogeneous accumulation of activity in the rat brain slices.

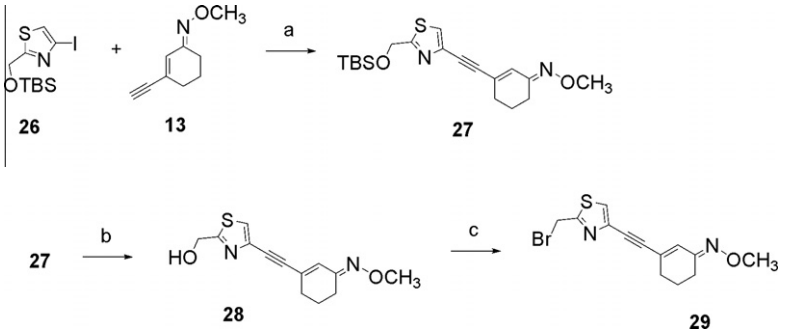

Scheme 4. Synthesis of the labeling precursor (*E*)-3-((2-(bromomethyl)thiazol-4-yl)ethynyl)cyclohex-2-enone *O*-methyl oxime (**29**). Reagents and conditions: (a) DMF, Et_3N, $Pd(PPh_3)_4$, CuI, rt, 24 h, ~91% (crude); (b) THF, TBAF in THF (1 M), rt, 50 min, 47%; (c) THF, CBr_4, $P(Ph)_3$, rt, 2 h, 28%.

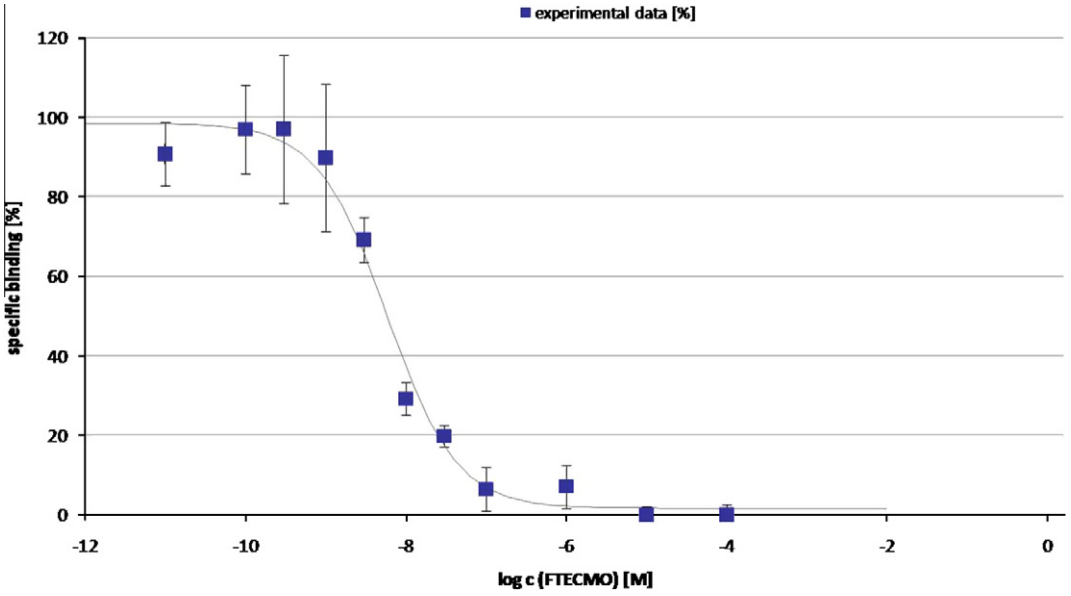

Figure 2. Displacement binding curve of FTECMO (**11**).

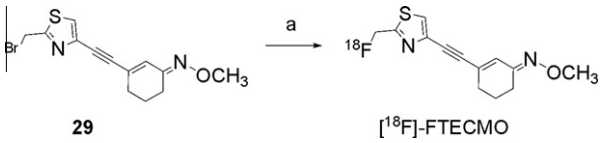

Scheme 5. Radiosynthesis of [^{18}F]-FTECMO. Reagents and conditions: (a) K[^{18}F]F-K2.2.2, ACN, 90 °C, 10 min.

2.7. PET study

PET studies in male Wistar rats (n = 3) were undertaken to analyze whether mGluR5-expressing regions in the rat brain could be visualized by [^{18}F]-FTECMO. Summed images for the total acquisition time of 60 min did not show any substantial brain uptake in the three rats tested. However, high skeletal accumulation of radioactivity was evident (Fig. 5). Region of interest (ROI) analysis

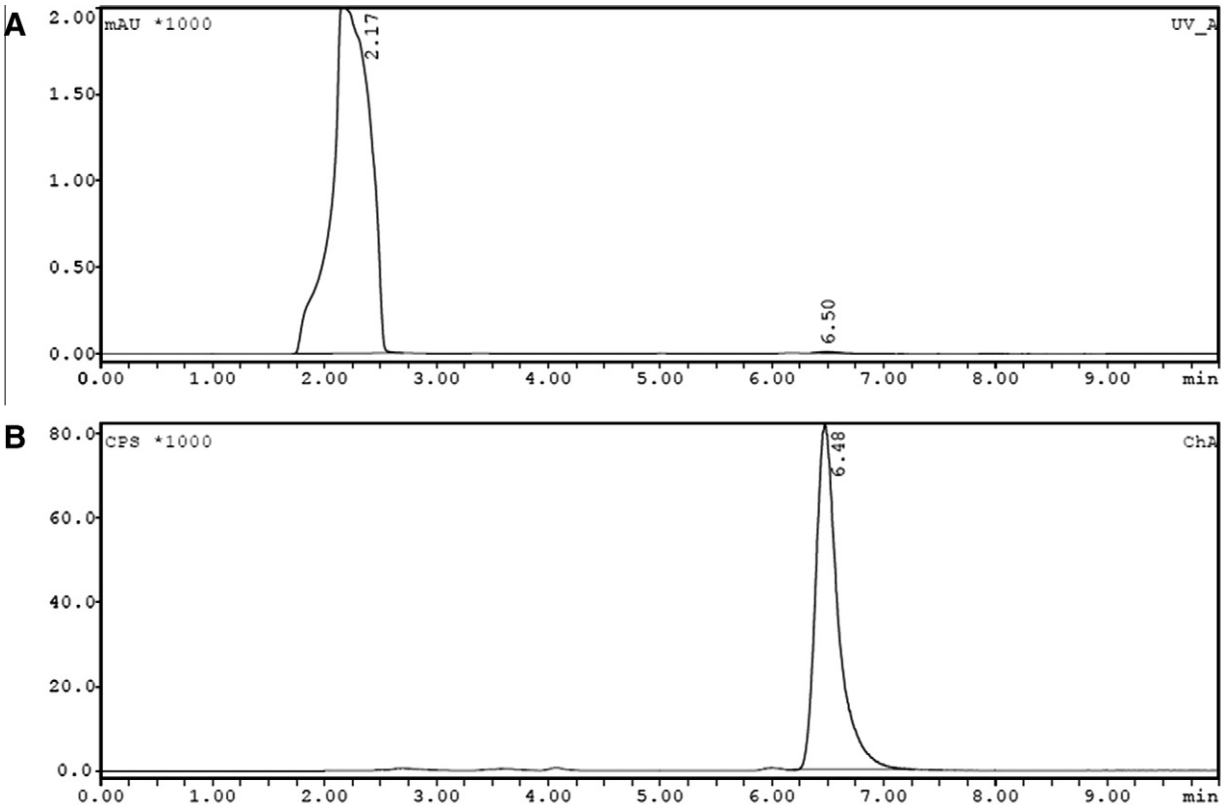

Figure 3. (A) UV HPLC profile of formulated [^{18}F]-FTECMO containing ascorbic acid (retention time = 2.17 min) (B) RadioHPLC profile of formulated [^{18}F]-FTECMO (retention time = 6.48 min).

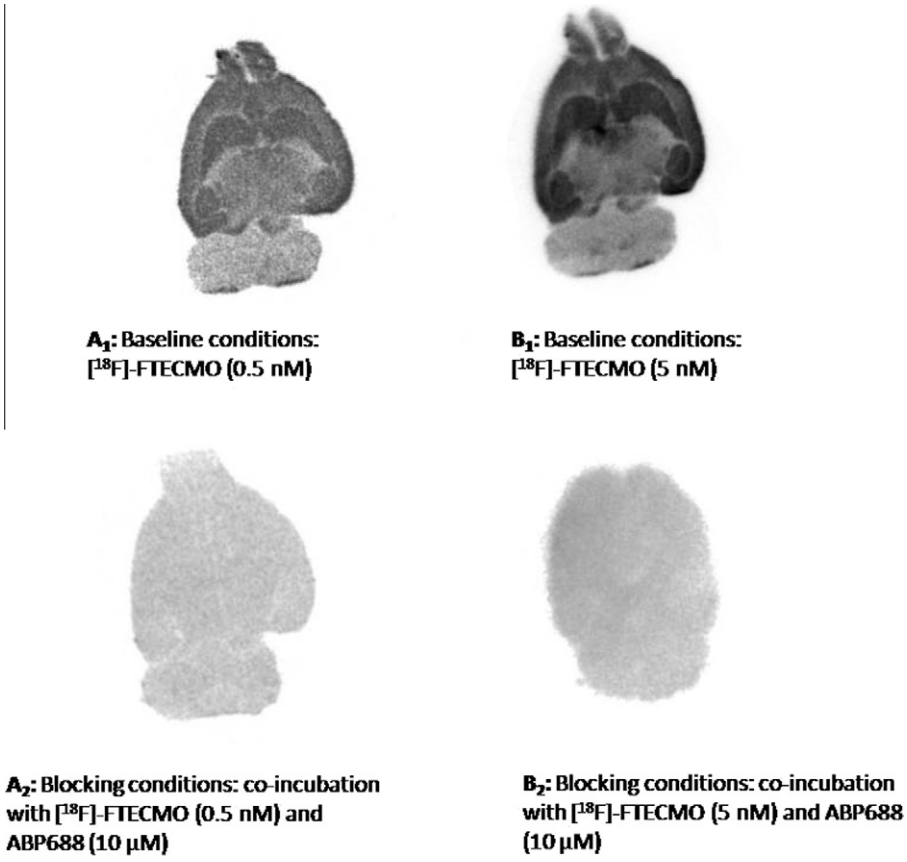

Figure 4. In vitro autoradiography of horizontal sections of rat brains incubated under baseline (A_1 and B_1) and blocking conditions (A_2 and B_2).

of dynamic PET data of two rats confirmed the high radioactivity uptake in the skeleton, which strongly increased during the scanning period (Figs. 5 and 6). Radioactivity uptake in the brain was low during the whole scan period. The dynamic data also showed that radioactivity accumulation was higher in the hindbrain than in the forebrain regions (cortex, striatum, hippocampus).

2.8. In vivo metabolism

Plasma samples were collected from the tail vein of a Wistar rat at 5 and 30 min after [^{18}F]-FTECMO iv injection. For both samples, two radioactivity peaks were identified by HPLC and UPLC. The first peak, which was absent before injection, appeared in the void volume, suggesting the in vivo formation of [^{18}F]-fluoride or another very hydrophilic radiometabolite. The second peak corresponded to [^{18}F]-FTECMO. It accounted for 60% (in the sample withdrawn at 5 min pi) and 31% (30 min pi) of the total radioactivity.

3. Discussion

MGluR5 has been shown to be involved in numerous central nervous system disorders. Non-invasive in vivo imaging of the receptor using PET can give further insight into the underlying pathophysiological processes and help understand mGluR5 pharmacology, which in turn will speed up drug development.[28,29] Efforts have been made in recent years to develop suitable mGluR5 PET tracers. However, to date only two mGluR5 PET ligands, [^{11}C]-ABP688 and [^{18}F]SP203, have been fully characterized in humans. Although [^{11}C]-ABP688 displays favorable in vivo imaging parameters, the labeling with the short-lived nuclide carbon-11

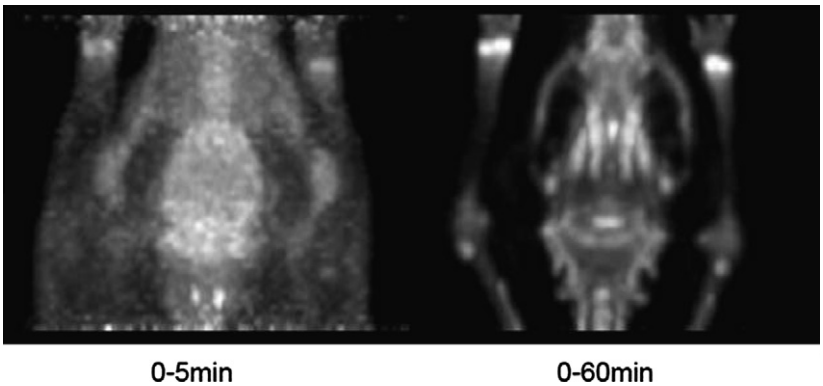

Figure 5. MIP (maximum intensity projection) PET images of a rat brain obtained with [^{18}F]-FTECMO.

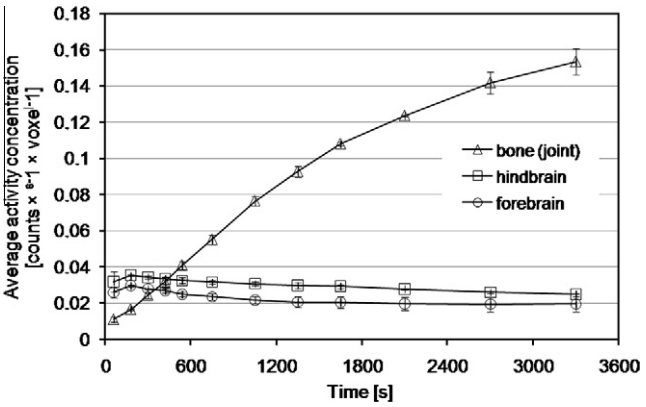

Figure 6. Time activity curves of [^{18}F]-FTECMO uptake. ROI analysis of dynamic PET scans from 0 to 60 min after i.v. injection of 30 MBq [^{18}F]-FTECMO into male Wistar rats. ROIs were defined for forebrain (cortex, striatum,hippocampus), hindbrain (including cerebellum) and bone (joint). Mean dose-normalized values of two independent experiments with error bars indicating the single values.

($t_{1/2}$ = 20 min) limits its widespread use. [^{18}F]SP203 showed species dependent in vivo defluorination in monkeys[20] and in rats,[30] that is, undesirable for in vivo imaging. However, enzymatic defluorination was negligible in human studies.[23,31]

With the hope of obtaining a fluorine-18 labeled PET tracer with structural elements of both [^{18}F]SP203 and [^{11}C]-ABP688, four novel thiazole containing ABP688 derivatives (**11**, **14**, **24**, and **25**) were synthesized and screened for their binding affinity towards mGluR5. Compound **14** does not contain a fluorine atom and served only as a model compound. Compound **11**, named FTECMO, exhibited a K_i value of 5.5 ± 1.4 nM which is comparable with the K_i value of 4.4 ± 1.0 nM for ABP688 obtained in a parallel displacement experiment. The replacement of the methyl-pyridine moiety in ABP688 with a fluoromethyl-thiazole moiety was obviously well tolerated by mGluR5. However, this does not hold true for compounds **24** and **25** (Table 1), analogues of compound **7.**[26] Compound **7** was previously shown to be a high affinity mGluR5 ligand. For these compounds, the binding affinities were reduced by 7- and 10-fold, respectively, when the pyridine ring was replaced with either a thiazole or a methylthiazole moiety. The more promising candidate FTECMO, with the highest binding affinity determined in this study, was selected for further evaluation as a potential PET tracer. A convenient one-step radiolabeling was established for [^{18}F]-FTECMO. Reacting the bromo-precursor **29** with K[^{18}F]F-K_{222} in acetonitrile at 90 °C afforded [^{18}F]-FTECMO in good radiochemical yields (up to 45%, decay corrected). Semi-preparative HPLC purification resulted in a highly pure product with a radiochemical purity greater than 97% (Fig. 3). Furthermore, high specific radioactivities ranging from 80 to 120 GBq/μmol were reproducibly obtained. The tracer was identified by co-injection with unlabeled FTECMO.

In vitro autoradiographical studies using rat brain slices revealed a heterogeneous and displaceable binding of [^{18}F]-FTECMO in brain regions such as the hippocampus, striatum, and cortex, regions known to contain high densities of mGluR5. In addition, [^{18}F]-FTECMO exhibited high stability in human and in rat plasma over 120 min. In rat liver microsomes, only minimal degradation was observed when UPLC analysis was performed. The short retention time in the UPLC system points to a very hydrophilic degradation product, which is presumably [^{18}F]-fluoride. The promising results of the stability studies and the positive in vitro results such as high binding affinity and displaceable accumulation of the tracer in rat brain slices prompted us to further evaluate [^{18}F]-FTECMO.

PET experiments were carried out in Wistar rats in order to evaluate the suitability of [^{18}F]-FTECMO in vivo. Despite an optimal log D of 1.6, low accumulation of [^{18}F]-FTECMO was observed in mGluR5-rich brain regions. In contrast, a strong accumulation of activity was observed in the bones, including the skull. ROI analysis of the dynamic PET data confirmed uptake of radioactivity into the bones and demonstrated that activity in the forebrain (cortex, striatum, hippocampus) and the hindbrain (including cerebellum) peaked at a low level immediately after radiotracer injection. Based on the distribution pattern of mGluR5 in the mammalian brain, radioactivity accumulation would be expected to be higher in the forebrain than in the hindbrain. However, in all the PET scans the uptake of radioactivity was higher in the hindbrain than in the forebrain regions.

Since metabolism studies revealed only one radioactive metabolite, which is presumably [^{18}F]-fluoride, it is unlikely that the higher uptake resulted from a metabolite. It is also unlikely that the higher accumulation in the hindbrain is derived from specific binding to a target other than mGluR5 since specific binding usually results in much higher uptake values and differently shaped time-activity curves. Moreover, the in vitro autoradiographic studies clearly indicated the specificity of [^{18}F]-FTECMO for mGluR5-rich brain regions when ABP688, a known ligand for mGluR5, was used as a blocking agent. Finally, the discrepancy may result from perfusion phenomena that cannot be properly addressed in a brain PET scan, that is, in addition flawed by accumulation of radioactivity in the skull. This high uptake of radioactivity in bones, including the skull and in particular joints is a strong evidence for in vivo radiodefluorination.[32] This is in agreement with our findings from the in vivo metabolism studies.

[^{18}F]-FPECMO, a fluoropyridine analogue of ABP688, similarly showed no clear-cut visualization of mGluR5-rich brain regions in rats. [^{18}F]-FPECMO was also rapidly defluorinated in vivo and resulted in radioactivity accumulation in bones and the skull.[24] The radioactivity uptake into rat brain after [^{18}F]-FPECMO injection peaked early after tracer injection but was eliminated from the fore- and hindbrain regions rapidly. In the present study [^{18}F]-FTECMO showed substantially a lower radioactivity peak. The visualization of mGluR5-rich brain regions with [^{18}F]-FTECMO in vivo was not only affected by radiodefluorination but it also failed, because radioactive uptake in the brain was not sufficient enough to yield a clear PET signal with an appropriate signal-to-background ratio even at early time points (Fig. 5). The lipophilicity of [^{18}F]-FTECMO ($\log D_{pH7.4}$ = 1.6 ± 0.2), however, suggests ideal physicochemical properties for diffusion through the blood–brain barrier.[33] The low brain uptake cannot be assigned exclusively to the rapid radiodefluorination of [^{18}F]-FTECMO, since the amount of remaining intact tracer—31% at 30 min pi—would be high enough for the visualization of mGluR5-rich brain regions. The in vivo metabolism of [^{11}C]-ABP688, for example, follows a similar time course with only 29% of parent tracer available at 30 min pi but still enables good PET imaging.[34] Presumably, [^{18}F]-FTECMO is hindered from passing the blood–brain barrier. The low penetration of [^{18}F]-FTECMO may be due to low passive diffusion across the cell membranes, although sufficient passive diffusion would be expected based on its log D at pH 7.4. Alternatively, blood–brain barrier penetration may be low because of efflux transport by P-glycoprotein[35] or another ABC transporter or a solute carrier.

Structurally, [^{18}F]-FTECMO is similar to [^{18}F]SP203. The enzymatic degradation of [^{18}F]SP203 was reported to occur in the rat brain and in the periphery, whereby the mechanism of radiodefluorination was shown to be mediated by glutathionylation through the glutathione-S-transferase system.[30] Glutathione-S-transferases are known to dehalogenate alkyl chlorides, bromides, and iodides.[36] Due to the structural similarity of the [^{18}F]-fluorothiazole moiety in both tracers and the absence of substantial defluorination in microsomes (no glutathione was added), we assume that the radiodefluorination in [^{18}F]-FTECMO is most likely derived from similar metabolic interactions.

It is noteworthy that in 2008, Brown et al.[23] described the successful in vivo imaging of [^{18}F]SP203 in humans, which was not hindered by in vivo defluorination. The striking species differences in defluorination were presumably the result of species differences in the expression, activity, and substrate selectivity of the mammalian glutathione-S-transferases.[37] In analogy to the metabolic profile of [^{18}F]SP203, the radiodefluorination of the [^{18}F]-fluoromethylthiazole moiety in [^{18}F]-FTECMO might be dramatically reduced in primates compared to rats and thus the evaluation of [^{18}F]-FTECMO in higher species such as monkeys and humans may be warranted once efflux transport at the blood–brain barrier is excluded.

4. Conclusion

In summary, the syntheses and investigation of four novel thiazole containing ABP688 analogues led to the identification of a high affinity ligand for mGluR5, FTECMO. Its radiolabeled analogue, [^{18}F]-FTECMO, represents a combination of structural elements from [^{18}F]SP203 and [^{11}C]-ABP688, that displayed favorable in vitro characteristics. [^{18}F]-FTECMO is however not suitable for mGluR5 imaging in vivo in rats. The further evaluation of [^{18}F]-FTECMO in higher species such as monkeys and humans may shed more light on the in vivo utility of this new PET ligand.

5. Experimental

5.1. General

Reagents and solvents utilized for experiments were obtained from commercial suppliers (Sigma–Aldrich, Alfa Aesar, Merck and Flucka) and were used without further purification unless stated otherwise. [^{3}H]-M-MPEP was provided by Novartis. Thin layer chromatography performed on pre-coated Silica Gel 60 F245 aluminum sheets suitable for UV absorption detection of compounds was used for monitoring reactions. Nuclear magnetic resonance spectra were recorded with a Bruker 400 MHz spectrometer with an internal standard from solvent signals. Chemical shifts are given in parts per million (ppm) relative to tetramethylsilane (0.00 ppm). Values of the coupling constant, *J*, are given in hertz (Hz). The following abbreviations are used for the description of ^{1}H NMR spectra: singlet (s), doublets (d), triplet (t), quartet (q), quintet (quint), doublet of doublets (dd), multiplet (m). The chemical shifts of complex multiplets are given as the range of their occurence. Low-resolution mass spectra (LR-MS) were recorded with a Micromass Quattro micro API LC-ESI. High-resolution mass spectra (HR-MS) were recorded with a Bruker FTMS 4.7T BioAPEXII (ESI). Quality control of the final products was performed on an Agilent 1100 system equipped with a radiodetector from Raytest using a reversed phase column (Gemini 10 μm C18, 300 × 3.9 mm, Phenomenex) by applying an isocratic solvent system with 70% MeCN in water and a flow of 1 mL/min. In vitro stability tests were performed on a Waters Acquitiy UPLC system (Berthold radiodetector) occupying an Acquitiy UPLC BEH C18 1.7 μm (2.1 × 50 mm) column. A binary solvent system with acetonitrile (solvent A) and water/acetonitrile (9:1) (solvent B) at a flow rate of 0.7 mL/min was used. During the first three minutes a gradient (100% B to 100% A) was applied followed by 0.5 min under isocratic conditions (100% A). The Swiss Federal Veterinary Office approved animal care and all experimental procedures.

5.2. Chemistry

5.2.1. 3-Bromocyclohex-2-enone *O*-methyl oxime (9)

O-Methylhydroxylamine hydrochloride (0.8 g, 9.4 mmol) was added to a solution of **8** (1.09 g, 6.27 mmol) in pyridine (20 mL). After stirring at rt for 18 h, 30 mL of H_2O were added and the reaction mixture was extracted with ether. The combined organic layers were washed with saturated $CuSO_4$ solution (3 × 30 mL) and brine (20 mL) and dried over Na_2SO_4. Evaporation led to 1.6 g of brown oil. Purification by flash column chromatography pentane/EtOAc (95:5) gave the *trans*-isomer as yellowish crystals (802 mg, 63%). *trans*-isomer: ^{1}H NMR (400 MHz, $CDCl_3$): δ 6.50 (s, 1H), 3.87 (s, 3H), 2.60 (t, J = 6.6 Hz, 2H), 2.52 (t, J = 6.3 Hz, 2H), 1.84 (quint, J = 4.1 Hz, 2H). MS *m*/*z* 203.85 (M+H)$^{+}$. *cis*-isomer: ^{1}H NMR (400 MHz, $CDCl_3$): δ 7.12 (s, 1H), 3.84 (s, 3H), 2.65 (t, J = 6.0 Hz, 2H), 2.36 (t, J = 6.0 Hz, 2H), 1.91 (quint, J = 6.6 Hz, 2H).

5.2.2. (*E*)-3-((2-(Fluoromethyl)thiazol-4-yl)ethynyl)cyclohex-2-enone *O*-methyl oxime (11)

Et_3N (0.5 mL) and CuI (7.7 mg, 0.04 mmol) were added under argon to a degassed solution of $Pd(PPh_3)_4$ (20.4 mg, 0.018 mmol) and **10** (110 mg, 0.54 mmol) in DMF (5 mL). TBAF (1.2 mmol; 1.0 M solution in THF, 1.2 mL) was added to a solution of 2-(fluoromethyl)-4-((trimethylsilyl)ethynyl)thiazole (85 mg, 0.6 mmol) in DMF (4 mL). After stirring for 30 min, the mixtures were combined and stirred for 20 h at rt. Sat. NH_4Cl solution (20 mL) was added and the resulting mixture was extracted with EtOAc (3 × 20 mL). The combined organic layers were washed with water (2 × 20 mL) and brine (10 mL) and dried over Na_2SO_4. Evaporation of the solvents under reduced pressure gave 370 mg of brown crude material. The crude product was purified twice by column chromatography with pentane/EtOAc (8:2) to afford compound **11** as brown crystals (17 mg, 11%). Mp: 58.5 °C. ^{1}H NMR (400 MHz, $CDCl_3$): δ 7.53 (s, 1H), 6.54 (s, 1H), 5.62 (d, J = 47.1 Hz, 2H), 3.92 (s, 3H), 2.54 (t, J = 6.3 Hz, 2H), 2.37 (t, J = 5.8 Hz, 2H), 1.79 (quint, J = 6.3 Hz, 2H). ^{13}C NMR (100 MHz, $CDCl_3$): δ 20.8, 22.2, 29.4, 62.0, 80.6 (d, J = 170.6 Hz), 86.0, 90.3, 123.9 (d, J = 2.7 Hz), 127.0, 130.6, 137.6, 155.3, 164.8 (d, J = 24.3 Hz). ^{19}F NMR (375 MHz, $CDCl_3$): δ −211.52. MS *m*/*z* 264.94 (M+H)$^{+}$. HRMS calcd for $C_{13}H_{13}FN_2OS$, 264.0728; found, 264.0728.

5.2.3. (*E*)-3-(Thiazol-2-ylethynyl)cyclohex-2-enone *O*-methyl oxime (14)

$Pd(PPh_3)_4$ (15 mg, 0.013 mmol) was added under argon to a degassed solution of 2-bromothiazole **12** (200 mg, 1.22 mmol) in DMF (2.5 mL). The mixture was stirred at rt for 5 min before Et_3N (1 mL) was added. The mixture was stirred for further 5 min before addition of CuI (6 mg, 0.03 mmol) and **13** (180 mg, 1.22 mmol), that was obtained as previously described.[26] The mixture was stirred at room temperature for 48 h, quenched with satd NH_4Cl (20 mL) and extracted with ether (3 × 20 mL). The combined organic layers were washed with water (2 × 20 mL) and brine (20 mL). The solvents were evaporated under reduced pressure and the residue was purified by column chromatography with pentane/EtOAc (9:1) to afford compound **14** as light yellow crystals (74 mg, 26%). Mp: 55.6 °C. ^{1}H NMR (400 MHz, $CDCl_3$): δ 7.61 (d, J = 3.2 Hz, 1H), 7.37 (d, J = 3.5 Hz, 1H), 6.60 (s, 1H), 3.93 (s, 3H), 2.55 (t, J = 6.0 Hz, 2H), 2.39 (t, J = 5.8 Hz, 2H), 1.81 (quint, J = 6.7 Hz, 2H). ^{13}C NMR (100 MHz, $CDCl_3$): δ 21.1, 22.4, 29.4, 62.5, 85.6, 94.9, 121.3, 126.6, 132.2, 144.1, 148.9, 155.4. MS *m*/*z* 232.94 [M^{+}, 100]. MS *m*/*z* 232.94 (M+H)$^{+}$. HRMS calcd for $C_{12}H_{13}N_2OS$, 233.0743; found, 233.0744.

5.2.4. *(E)*-3-(Thiazol-4-ylethynyl)cyclohex-2-enone oxime (18)

Compound **18** was prepared in an analogous way to compound **14**. Starting from **15** (1000 mg, 6.1 mmol) and **17** (840 mg, 6.2 mmol) compound **18** was obtained as yellow crystals (720 mg, 54%). The product was purified by column chromatography using pentane/EtOAc (1:1) as the mobile phase. ^{1}H NMR (400 MHz, $CDCl_3$): δ 8.80 (s, 1H), 7.53 (s, 1H), 6.61 (s, 1H), 2.63 (t, J = 6.8 Hz, 2H), 2.40 (t, J = 5.7 Hz, 2H), 1.83 (quint, J = 6.2 Hz, 2H).

^{13}C NMR (100 MHz, $CDCl_3$): δ 20.7, 21.6, 29.3, 86.4, 90.3, 122.4, 127.6, 130.4, 138.3, 152.8, 156.3. MS *m*/*z* 218.82 $(M+H)^+$.

5.2.5. (*E*)-3-((2-Methylthiazol-4-yl)ethynyl)cyclohex-2-enone oxime (19)

This compound was prepared analogously to compound **18**. Starting from **16** (790 mg, 4.44 mmol) and **17** (600 mg, 4.44 mmol), compound **19** was obtained as yellow crystals (248 mg, 24%). Mp: 147.8–148.4 °C. ^{1}H NMR (400 MHz, $CDCl_3$): δ 7.21 (s, 1H), 6.59 (s, 1H), 2.73 (s, 3H), 2.64 (t, *J* = 6.1 Hz, 2H), 2.41 (t, *J* = 6.2 Hz, 2H), 1.83 (quint, *J* = 6.3 Hz, 2H). ^{13}C NMR (100 MHz, $CDCl_3$): δ 19.2, 20.6, 21.6, 29.4, 86.6, 89.4, 122.9, 125.4, 129.3, 136.6, 156.6, 165.9. MS *m*/*z* 232.82 $(M+H)^+$. HRMS calcld for $C_{12}H_{12}N_2OS$, 232.0670; found, 232.0665.

5.2.6. (*E*)-3-(Thiazol-4-ylethynyl)cyclohex-2-enone *O*-2-(2-(*tert*-butyldimethylsilyloxy)ethoxy)ethyl oxime (20)

To a solution of **18** (250 mg, 1.15 mmol) in DMF (21 mL) was added 60% NaH (90 mg, 2.25 mmol). After stirring for 30 min at rt, (2-(2-bromoethoxy)ethoxy)(*tert*-butyl)dimethylsilane (340 mg, 1.2 mmol) was added. The reaction mixture was stirred for 1.5 h and then quenched by addition of a 50% $NaHCO_3$ solution (15 mL). The mixture was extracted with ether (3 × 20 mL). The combined organic layers were washed with water (2 × 20 mL) and brine (20 mL) and dried over Na_2SO_4. The solvents were evaporated under reduced pressure and the obtained crude product was purified by column chromatography with pentane/EtOAc (6:4) to give compound **20** as a slightly yellow oil (390 mg, 80%). ^{1}H NMR (400 MHz, $CDCl_3$): δ 8.78 (s, 1H), 7.51 (s, 1H), 6.53 (s, 1H), 4.25 (t, *J* = 5.4 Hz, 2H), 3.76 (q, *J* = 5.40 Hz, 4H), 3.56 (t, *J* = 4.9 Hz, 2H), 2.57 (t, *J* = 7.0 Hz, 2H), 2.38 (t, *J* = 6.5 Hz, 2H), 1.79 (quint, *J* = 7.0 Hz, 2H), 0.89 (s, 9H), 0.06 (s, 6H). ^{13}C NMR (100 MHz, $CDCl_3$): δ −5.3, 18.4, 20.8, 22.3, 25.9, 29.4, 62.8, 69.7, 72.7, 73.7, 86.3, 90.3, 122.4, 127.2, 130.5, 138.4, 152.6, 155.6. MS *m*/*z* 420.90 $(M+H)^+$. HRMS calcld for $C_{21}H_{32}N_2NaO_3SSi$, 443.1795; found, 443.1805.

5.2.7. (*E*)-3-((2-Methylthiazol-4-yl)ethynyl)cyclohex-2-enone *O*-2-(2-(*tert*-butyldimethylsilyloxy)ethoxy)ethyl oxime (21)

This compound was prepared analogously to compound **20**. Starting from **19** (233 mg, 1.0 mmol) and 2-(2-bromoethoxy)(*t*-butyl)dimethylsilane (348 mg, 1.2 mmol), compound **21** was obtained as a clear oil (315 mg, 72%). ^{1}H NMR (400 MHz, $CDCl_3$): δ 7.31 (s, 1H), 6.51 (s, 1H), 4.25 (t, *J* = 5.0 Hz, 2H), 3.78–3.73 (m, 4H), 3.56 (t, *J* = 5.1 Hz, 2H), 2.72 (s, 3H), 2.56 (t, *J* = 6.1 Hz, 2H), 2.37 (t, *J* = 5.7 Hz, 2H), 1.78 (quint, *J* = 6.8 Hz, 2H), 0.89 (s, 9H), 0.07 (s, 6H). ^{13}C NMR (100 MHz, $CDCl_3$): δ −5.3, 18.4, 19.2, 20.8, 22.3, 25.9, 29.4, 62.8, 69.8, 72.7, 73.7, 86.6, 89.7, 122.5, 127.3, 130.3, 136.7, 155.7, 165.8. MS *m*/*z* 434.96 $(M+H)^+$. HRMS calcd for $C_{22}H_{35}N_2O_3SSi^+$, 435.2132; found, 435.2139.

5.2.8. (*E*)-2-(2-(3-(Thiazol-4-ylethynyl)cyclohex-2-enylideneaminooxy)ethoxy)ethyl 4-methylbenzenesulfonate (22)

To a solution of **20** (363 mg, 0.86 mmol) in THF (22 mL) was added TBAF trihydrate (680 mg, 2.15 mmol). After stirring the mixture for 1.5 h at rt, water (15 mL) was added. The solution was extracted with EtOAc and the organic layers were washed with water and brine and dried over Na_2SO_4. Evaporation of solvents under reduced pressure led to an orange crude product which was used directly without further purification. To the solution of (*E*)-3-(thiazol-4-ylethynyl)cyclohex-2-enone *O*-2-(2-hydroxyethoxy)-ethyl oxime (crude = 338 mg) in dry CH_2Cl_2 (6 mL) was added Et_3N (312 μL). The mixture was cooled to 0 °C and then treated with toluenesulfonylchloride (401 mg, 1.3 mmol). After stirring at rt for 8 h, the mixture was diluted with water (25 mL) and extracted with ether (3 × 20 mL). The combined organic layer was washed with water (2 × 20 mL) and brine (20 mL), dried over Na_2SO_4 and the solvents were evaporated under reduced pressure. The residue was purified by column chromatography with pentane/Et_2O (1:4) to give pure **22** as a yellow oil (360 mg, 91%). ^{1}H NMR (400 MHz, $CDCl_3$): δ 8.78 (s, 1H), 7.80 (d, *J* = 8.3 Hz, 2H), 7.52 (s, 1H), 7.34 (d, *J* = 10.2 Hz, 2H), 6.52 (s, 1H), 4.20–4.14 (m, 4H), 3.72–3.65 (m, 4H), 2.55 (t, *J* = 6.8 Hz, 2H), 2.44 (s, 3H), 2.38 (t, *J* = 5.2 Hz, 2H), 1.79 (quint, *J* = 6.6 Hz, 2H). ^{13}C NMR (100 MHz, $CDCl_3$): δ 20.8, 21.6, 22.3, 29.3, 68.7, 69.2, 69.8, 73.4, 86.4, 90.3, 122.4, 127.5, 128.0, 129.8, 130.3, 133.1, 138,4, 144.8, 152.6, 155.8. MS *m*/*z* 482.71 $(M+Na)^+$. HRMS calcld for $C_{22}H_{24}N_2NaO_5S_2$, 483.1019; found, 483.1012.

5.2.9. (*E*)-2-(2-(3-((2-Methylthiazol-4-yl)ethynyl)cyclohex-2-enylideneaminooxy)ethoxy)ethyl 4-methylbenzenesulfonate (23)

This compound was synthesized in analogy to compound **22**. Starting from **21** (290 mg, 0.66 mmol), compound **23** was obtained as a yellow oil (270 mg, 85%). ^{1}H NMR (400 MHz, $CDCl_3$): δ 7.80 (d, *J* = 8.1 Hz, 2H), 7.33 (d, *J* = 8.1 Hz, 1H), 7.31 (s, 1H), 6.49 (s, 1H), 4.18–4.14 (m, 4H), 3.70–3.65 (m, 4H), 2.72 (s, 3H), 2.53 (t, *J* = 6.5 Hz, 2H), 2.44 (s, 3H), 2.36 (t, *J* = 6.5 Hz, 2H), 1.78 (quint, *J* = 6.5 Hz, 2H). ^{13}C NMR (100 MHz, $CDCl_3$): δ 19.2, 20.8, 21.6, 22.3, 29.4, 68.7, 69.2, 69.8, 73.4, 86.8, 89.6, 122.6, 127.6, 128.0, 129.8, 130.1, 133.1, 136.7, 144.8, 155.9, 165.8. MS *m*/*z* 474.84 $(M+H)^+$. HRMS calcd for $C_{23}H_{26}N_2O_5S_2H^+$, 475.1356; found, 475.1356.

5.2.10. (*E*)-3-(Thiazol-4-ylethynyl)cyclohex-2-enone *O*-2-(2-fluoroethoxy)ethyl oxime (24)

Hydrated TBAF (280 mg, 0.89 mmol) was dried under high vacuum at 45 °C for 24 h and was then dissolved in dry THF (10 mL). A solution of **22** (180 mg, 0.4 mmol) in dry THF (5 mL) was added. After stirring the mixture for 5 h at 60 °C, water (10 mL) was added. The solution was extracted with ether (3 × 20 mL). The organic layers were washed with water (2 × 20 mL) and brine (20 mL) and dried over Na_2SO_4. After evaporation of the solvents, the brown crude product was purified by column chromatography with Et_2O/pentane (6:1) to give compound **24** as a clear oil (26 mg, 21%). ^{1}H NMR (400 MHz, $CDCl_3$): δ 8.78 (s, 1H), 7.52 (s, 1H), 6.53 (s, 1H), 4.62 (t, *J* = 4.1 Hz, 1H), 4.50 (t, *J* = 4.2 Hz, 1H), 4.27 (t, *J* = 5.1 Hz, 2H), 3.81–3.76 (m, 3H), 3.71 (t, *J* = 3.3 Hz, 1H), 2.57 (t, *J* = 6.8 Hz, 2H), 2.38 (t, *J* = 6.3 Hz, 2H), 1.80 (quint, *J* = 6.6 Hz, 2H). ^{13}C NMR (100 MHz, $CDCl_3$): δ 20.8, 22.3, 29.4, 69.8, 70.3 (d, *J* = 19.4 Hz), 73.5, 83.1 (d, *J* = 169.1 Hz), 86.3, 90.3, 122.4, 127.4, 130.4, 138.4, 152.6, 155.8. ^{19}F NMR (376 MHz, $CDCl_3$): δ −223.09. MS *m*/*z* 308.80 $(M+H)^+$.

5.2.11. (*E*)-3-((2-Methylthiazol-4-yl)ethynyl)cyclohex-2-enone *O*-2-(2-fluoroethoxy)ethyl oxime (25)

This compound was obtained in an analogous way to **24**. Starting material **23** (150 mg, 0.32 mmol) gave a slightly yellow oil (39 mg, 40%). ^{1}H NMR (400 MHz, $CDCl_3$): δ 7.31 (s, 1H), 6.50 (s, 1H), 4.62 (t, *J* = 4.4 Hz, 1H), 4.50 (t, *J* = 3.9 Hz, 1H), 4.26 (t, *J* = 5.1 Hz, 2H), 3.8 (t, *J* = 4.1 Hz, 3H), 3.71 (t, *J* = 4.3 Hz, 1H), 2.71 (s, 3H), 2.56 (t, *J* = 6.36 Hz, 2H), 2.36 (t, *J* = 7.0 Hz, 2H), 1.78 (quint, *J* = 6.2 Hz, 2H). ^{13}C NMR (100 MHz, $CDCl_3$): δ 19.2, 20.8, 22.3, 29.4, 69.9, 70.3 (d, *J* = 20.5 Hz), 73.5, 83.0 (d, *J* = 169.1 Hz), 86.8, 89.6, 122.5, 127.5, 130.2, 136.7, 155.8, 165.8. ^{19}F NMR (376 MHz, $CDCl_3$): δ −223.11. MS *m*/*z* 322.77 $(M+H)^+$. HRMS calcd for $C_{16}H_{19}FN_2NaO_2S^+$, 345.1044; found, 345.1044.

5.2.12. (*E*)-3-((2-((*tert*-Butyldimethylsilyloxy)methyl)thiazol-4-yl)ethynyl)cyclohex-2-enone *O*-methyl oxime (27)

Compound **27** was prepared in an analogous way to compound **14**. Starting from **13** (430 mg, 2.88 mmol) and **26** (950 mg, 2.67 mmol) compound **27** was obtained (720 mg, 54%).

Purification by silica gel flash column chromatography with pentane/Et_2O (9:1) led to a mixture containing the desired product. It was used without further purification.

5.2.13. (*E*)-3-((2-(Hydroxymethyl)thiazol-4-yl)ethynyl)cyclohex-2-enone *O*-methyl oxime (28)

To a solution of **27** containing impurities (920 mg, 2.443 mmol) in THF (25.5 mL) was added a solution of TBAF (1 M) in THF (2.95 mL, 2.923 mmol). After stirring the mixture for 1 h at rt the reaction was quenched with water (20 mL). The mixture was extracted with EtOAc (3 × 20 mL) and the combined organic layers were washed with water (2 × 20 mL) and brine (20 mL) and dried with Na_2SO_4. The solvents were evaporated under reduced pressure and the residue was purified by flash column chromatography with pentane/EtOAc (6:4) to give the desired alcohol **28** (304 mg, yield = 47%). ^{1}H NMR (400 MHz, $CDCl_3$): δ 7.43 (s, 1H), 6.49 (s, 1H), 4.94 (s, 1H), 3.90 (s, 3H), 3.36 (s, 1H), 2.52 (t, J = 6.5 Hz, 2H), 2.35 (t, J = 6.0 Hz, 2H), 1.78 (quint, J = 6.5 Hz, 2H). ^{13}C NMR (100 MHz, $CDCl_3$): δ 20.8, 22.1, 29.4, 62.0, 62.1, 86.5, 90.0, 123.0, 127.2, 130.3, 137.1, 155.4171.5. MS m/z 263.02 $(M+H)^+$. HRMS calcd for $[M^+]$ $C_{13}H_{14}FN_2O_2S^+$, 262.0771; found: 262.0768.

5.2.14. (*E*)-3-((2-(Bromomethyl)thiazol-4-yl)ethynyl)cyclohex-2-enone *O*-methyl oxime (29)

A solution of alcohol **28** (261 mg, 0.995 mmol) in benzene (9.5 mL) was cooled to 0 °C and CBr_4 (1.661 mg, 5.024 mmol) and triphenylphosphine (1.312 mg, 5.0 mmol) were added. The mixture was allowed to warm up to rt and stirred for 2 h. Then the reaction mixture was filtered over Celite and the solvents were evaporated under reduced pressure. Flash column chromatography with hexane/EtOAc (5:1) as the mobile phase gave **29** as a beige solid (89 mg, 30%). Mp: 78.9–79.2 °C. ^{1}H NMR (400 MHz, $CDCl_3$): δ 7.49 (s, 1H), 6.52 (s, 1H), 4.70 (s, 2H), 3.91 (s, 3H), 2.53 (t, J = 6.4 Hz, 2H), 2.37 (t, J = 6.2 Hz, 2H), 1.79 (quint, J = 6.5 Hz, 2H). ^{13}C NMR (100 MHz, $CDCl_3$): δ 20.8, 22.1, 26.2, 29.3, 62.0, 86.1, 90.1, 124.8, 127.0, 130.6, 137.5, 155.3, 165.7. MS m/z 326.92 $(M+H)^+$. HRMS calcd for $[M^+]$ $C_{13}H_{13}BrN_2OS^+$, 323.9927; found: 323.9930.

5.3. In vitro binding assays

5.3.1. Preparation of membranes

Sprague Dawley rats were sacrificed by decapitation and the brains were harvested immediately. After removal of the cerebellum the brain material was homogenized in 10 volumes of ice-cold sucrose buffer (0.32 M sucrose; 10 mM Tris/acetate buffer pH 7.4) with a polytron (PT-1200 C, Kinematica AG) for 1 min at setting 4. The obtained homogenate was centrifuged (1000g, 15 min, 4 °C) and the supernatant containing the membranes was removed and kept while the pellet was resuspended in five volumes of sucrose buffer. After a second round of homogenization and centrifugation, the two supernatants were combined and centrifuged at 17,000g for 20 min at 4 °C to pellet the membranes. The pellet was resuspended with incubation buffer (5 mM Tris/acetate buffer, pH 7.4) and centrifuged again at 17,000g, (20 min, 4 °C) followed by resuspension of the sedimented membranes with incubation buffer. The final membrane suspension was stored in aliquots at −70 °C. For each assay the required amount of membrane preparation was thawed and kept on ice during all preparation processes. The protein concentration was determined with a Bio-Rad Microassay with bovine serum albumin as a standard protein (Bradford, 1976).[38]

5.3.2. Displacement assays

For all four novel ligands (**11**, **14**, **24** and **25**) the binding affinity was determined by displacement assays using [^{3}H]-M-MPEP (2 nM) as a radioligand. The membranes (see above) were incubated with increasing concentrations of the test compound (1 pM to 100 μM), each in triplicate, in incubation buffer II (30 mM NaHEPES, 110 mM NaCl, 5 mM KCl, 2.5 mM $CaCl_2 \times H_20$, 1.2 mM $MgCl_2$, pH 8). Non-specific binding was determined in the presence of ABP688 (100 μM). The test samples with a total volume of 200 μL were incubated for 45 min at rt. For the removal of free radioligand, 4 mL of ice-cold incubation buffer II were added followed by vacuum filtration over GF/C filters (Whatman) that were previously impregnated with poly(ethyleneimine) 0.05% (Fluka #03880, Switzerland). After rinsing the filters twice with 4 mL of ice-cold buffer II, the filters were transferred to 4 mL scintillation-liquid (Ultima Gold, Perkin Elmer) in beta scintillation vials. Radioactivity retained on the filters was measured by beta counting (Liquid Scintillation Analyser 1900TR, Canberra Packard). Data was evaluated with KELL Radlig Software (Biosoft). For calculation of the K_i value, the Cheng–Prusoff equation was applied, with a K_D value of 2.0 nM for [^{3}H]-M-MPEP.

5.4. Radiosynthesis of [^{18}F]-FTECMO

The conversion of **29** into [^{18}F]-FTECMO was achieved via nucleophilic substitution with [^{18}F]-fluoride. [^{18}F]-fluoride was obtained via the ^{18}O(p,n)^{18}F reaction using 98% enriched ^{18}O-water. $^{18}F^-$ was trapped from the aqueous solution on a light QMA cartridge (Waters), which was previously preconditioned with 0.5 M K_2CO_3 (5 mL) and water (5 mL). A volume of 1 mL of Kryptofix $K_{2.2.2.}$ solution (Kryptofix $K_{2.2.2.}$; 2.5 mg, K_2CO_3, 0.5 mg in MeCN/water (3:1)) was used for the elution of $^{18}F^-$ from the cartridge. The solvents were evaporated at 110 °C under vacuum in the presence of slight inflow of nitrogen gas. After addition of acetonitrile (1 mL), azeotropic drying was carried out. This procedure was repeated twice and gave rise to dry $K_{2.2.2.}$–K[^{18}F] F complex. Already 15 min after end of bombardment a solution of precursor **30** (2 mg in 300 μL of dry acetonitrile) was added to the dried $K_{2.2.2.}$–K[^{18}F] F complex. The reaction mixture was heated at 90 °C for 10 min, followed by the addition of 50% MeCN in water (2 mL). Purification by semipreparative HPLC was carried out on a HPLC system equipped with a Merck-Hitachi L-6200A intelligent pump, a Knauer Variable Wavelength Monitor UV detector and a Geiger Müller LND 714 counter with Eberlein RM-14 instrument using a reversed phase column (Gemini 5μ C18, 250 × 10 mm, Phenomenex) with a solvent system and gradient as follows: H_2O (solvent A), acetonitrile (solvent B); flow 5 mL/min; 0–10 min: 10% B, 10–20 min: 10–50% B, 20–30 min: 50% B. [^{18}F]-FTECMO was eluted approximately 50 min after end of bombardment and ascorbic acid (16 mg) was added to the fraction containing [^{18}F]-FTECMO before the mixture was diluted with water (30 mL). The product was trapped on a C18 light SepPak cartridge (Waters), which was preconditioned with ethanol (5 mL) and water (5 mL). After washing the cartridge with 10 mL of water for removal of traces of acetonitrile, the product was eluted with 0.5 mL of ethanol through a sterile filter (0.2 μm). In order to obtain an injectable solution, the fraction was diluted with sterile saline water (9.5 mL) containing ascorbic acid (1 mg/mL). Determination of relative lipophilicity, radiochemical purity and specific activity was carried out during the quality control step. Identification of [^{18}F]-FTECMO was achieved by co-injection of reference **11**.

5.5. Determination of log $D_{pH7.4}$

The shake flask method[27] was performed (n = 5) with 0.5 mL of 1-octanol saturated with phosphate buffer (pH 7.4) and 0.5 mL of phosphate buffer (pH 7.4) saturated with 1-octanol. After addition of 20 μL of [^{18}F]-FTECMO solution (80 kBq) the samples were mixed for 15 min and then centrifuged at 5000g for 5 min before

the radioactivity in each phase was determined using a gamma counter (Wizard, Perkin Elmer).

5.6. In vitro stability tests

For the determination of the in vitro plasma stability of the radioligand, 13.5 μL of [^{18}F]-FTECMO in ethanol were added to human and rodent plasma (386.5 μL). The solutions were incubated for 120 min at 37 °C. At five different time points (0, 30, 60, 90, and 120 min) aliquots (70 μL) were taken and transferred into ice-cold acetonitrile (140 μL). After 10 min of centrifugation (5000*g*, 4 °C), the supernatant was analyzed by UPLC applying the conditions described above.

[^{18}F]-FTECMO microsomal stability was investigated employing pooled rat liver microsomes (BD Bioscience). The test compound (20–50 nM) or 15 μM testosterone (positive control), was preincubated for 5 min with 10 mM NADPH in 0.1 M phosphate buffer (pH 7.4) at 37 °C before addition of the microsome suspension (0.52 mg/mL protein) or a suspension of boiled microsomes as a negative control. At four different time points (0, 15, 30, and 60 min) 150 μL of ice-cold acetonitrile were added in order to precipitate all active enzymes. The samples were centrifuged at 5000*g* for 5 min to obtain the supernatant to be analyzed by UPLC as described.

5.7. In vitro autoradiography

The experiments were carried out with rat brain slices of male Sprague Dawley rats. The rats were sacrificed by decapitation and the brains were removed quickly and frozen in 2-methylbutane (Fluka) at −30 to −36 °C. Horizontal brain slices (10 μm) were obtained by cutting the brains at −20 °C with a Cryostate microtome HM 505 N (Microm). The slices were absorbed on SuperFrost slides (Menzel) and stored at −80 °C until used. For the experiment, the slices were allowed to thaw at rt for 30 min before incubation in HEPES–BSA buffer (30 mM Na-HEPES, 110 mM NaCl, 5 mM KCl, 2.5 mM $CaCl_2 \times H_2O$, 1.2 mM $MgCl_2$, 0.1% BSA, pH 7.4) at 4 °C for 10 min. The brain slice was then dripped with 300 μL of a [^{18}F]-FTECMO solution (0.5 nM or 5 nM, respectively) and incubated for 45 min at rt in a humid chamber. For blockade conditions, the brain slices were dripped with 300 μL of a mixture of unlabeled ABP688 and [^{18}F]-FTECMO (10 μM ABP688, 0.5 nM or 5 nM, respectively, [^{18}F]-FTECMO) and incubated in the same way for 45 min. After decanting the supernatant tracer solution, the brain slices were washed with HEPES buffer for 3 min (3×) and with distilled water for 5 s (2×) at 4 °C. A drying step at rt (40 min) was followed by exposition (7 min) of the brain tissue to appropriate phosphor imager plates (AGFA) and scanning in a BAS5000 reader (Fuji).

5.8. In vivo PET imaging

Animal care and all experimental procedures were approved by the Cantonal Veterinary Office of Zurich. Three adult male Wistar rats (436; 264 and 272 g) were obtained from Charles River (Sulzfeld, Germany) and were allowed free access to food and water. PET scanning was performed using the GE VISTA PET/CT tomograph, which is characterized by high sensitivity but a limited axial field-of-view of 4.8 cm.[39] The animals were immobilized by an isoflurane inhalation anesthesia and fixed on the bed of the tomograph before tracer injection. Monitoring of anesthesia during scanning was performed according to protocols published previously.[40] The animals were injected intravenously with [^{18}F]-FTECMO (25–30 MBq, 0.138–0.558 nmol) and scanned in a single bed position (setting the brain in the center of the field-of-view) with a dynamic PET acquisition mode for 60 min. Raw data were acquired in list-mode and reconstructed in user-defined time frames (dynamic: 5×2, 4×5, 3×10 min, two animals; static: 1×60 min, three animals) with a voxel size of $0.3775 \times 0.3775 \times 0.775$ mm and a matrix size of $175 \times 175 \times 61$. Image files were evaluated by region-of-interest (ROI) analysis using the dedicated software PMOD.[41]

5.9. In vivo metabolism

For the determination of in vivo radiometabolites a male Wistar rat was injected with [^{18}F]-FTECMO via a lateral tail vein (160 μL, 200 MBq). Blood samples were withdrawn from the opposite vein at 5 and 30 min post-injection. Whole blood was collected in heparin-coated tubes (BD Vacutainers) and centrifuged at 5000*g* for 5 min. The proteins of the supernatant plasma were precipitated by addition of an equal volume of acetonitrile and centrifuged at 5000*g* for 5 min. The supernatant was analyzed by analytical HPLC and UPLC.

Acknowledgments

We acknowledge the technical support of Claudia Keller, Petra Wirth and Mathias Nobst. We thank Christophe Lucatelli and Harriet Struthers for fruitful discussion.

References and notes

1. Ritzén, A.; Mathiesan, M. J.; Thomsen, C. *Basic Clin. Pharmacol.* **2005**, *97*, 202.
2. Conn, P. J.; Pin, J.-P. *Ann. Rev. Pharmacol.* **1997**, *37*, 205.
3. Shigemoto, R.; Nomura, S.; Ohishi, H.; Sugihara, H.; Nakanishi, S.; Mizuno, N. *Neurosci. Lett.* **1993**, *163*, 53.
4. Bruno, V.; Ksiazek, I.; Battaglia, G.; Lukic, S.; Leonhardt, T.; Sauer, D.; Gasparini, F.; Kuhn, R.; Nicoletti, F.; Flor, P. J. *Neuropharmacology* **2000**, *39*, 2223.
5. Wang, Q.; Walsh, D. M.; Rowan, M. J.; Selkoe, D. J.; Anwyl, R. *J. Neurosci.* **2004**, *24*, 3370.
6. Rouse, S. T.; Marino, M. J.; Bradley, S. R.; Awad, H.; Wittmann, M.; Conn, P. J. *Pharmacol. Ther.* **2000**, *88*, 427.
7. Ossowska, K.; Konieczny, J.; Wardas, J.; Pietraszek, M.; Kuter, K.; Wolfarth, S.; Pilc, A. *Amino Acids* **2007**, *32*, 179.
8. Palucha, A.; Branski, P.; Szewczyk, B.; Wieronska, J. M.; Klak, K.; Pilc, A. *Pharmacol. Biochem. Behav.* **2005**, *81*, 901.
9. Pilc, A.; Klodzinska, A.; Branski, P.; Nowak, G.; Palucha, A.; Szewczyk, B.; Tatarczynska, E.; Chojnacka-Wójcik, E.; Wieronska, J. M. *Neuropharmacology* **2002**, *43*, 181.
10. Ohnuma, T.; Augood, S. J.; Arai, H.; McKenna, P. J.; Emson, P. C. *Mol. Brain Res.* **1998**, *56*, 207.
11. Pietraszek, T.; Berghe, C. V. *Lec. Notes Comput. Sci.* **2006**, *3858*, 124.
12. Cosford, N. D. P.; Tehrani, L.; Roppe, J.; Schweiger, E.; Smith, N. D.; Anderson, J.; Bristow, L.; Brodkin, J.; Jiang, X. H.; McDonald, I.; Rao, S.; Washburn, M.; Varney, M. A. *J. Med. Chem.* **2003**, *46*, 204.
13. Gasparini, F.; Lingenhöhl, K.; Stoehr, N.; Flor, P. J.; Heinrich, M.; Vranesic, I.; Biollaz, M.; Allgeier, H.; Heckendorn, R.; Urwyler, S.; Varney, M. A.; Johnson, E. C.; Hess, S. D.; Rao, S. P.; Sacaan, A. I.; Santori, E. M.; Veliçelebi, G.; Kuhn, R. *Neuropharmacology* **1999**, *38*, 1493.
14. Chiamulera, C.; Epping-Jordan, M. P.; Zocchi, A.; Marcon, C.; Cottiny, C. C.; Tacconi, S.; Corsi, M.; Orzi, F.; Conquet, F. o. *Nat. Neurosci.* **2001**, *4*, 873.
15. Todd, P. K.; Mack, K. J.; Malter, J. S. *Proc. Natl. Acad. Sci. U.S.A.* **2003**, *100*, 14374.
16. Bordi, F.; Ugolini, A. *Prog. Neurobiol.* **1999**, *59*, 55.
17. Ametamey, S. M.; Treyer, V.; Streffer, J.; Wyss, M. T.; Schmidt, M.; Blagoev, M.; Hintermann, S.; Auberson, Y.; Gasparini, F.; Fischer, U. C.; Buck, A. *J. Nucl. Med.* **2007**, *48*, 247.
18. Hamill, T. G.; Krause, S. R. C.; Bonnefous, C.; Govek, S.; Seiders, T. G.; Cosford, N. P. D.; Roppe, J.; Kamenecka, T.; Patel, S.; Gibson, R. E.; Sanabria, S.; Riffel, K.; Eng, W.; King, C.; Yang, X.; Green, M. D.; O'malley, S. S.; Hargreaves, R.; Burns, H. D. *Synapse* **2005**, *56*, 205.
19. Patel, S.; Hamill, T. G.; Connolly, B.; Jagoda, E.; Li, W.; Gibson, R. E. *Nucl. Med. Biol.* **2007**, *34*, 1009.
20. Siméon, F. G.; Brown, A. K.; Zoghbi, S. S.; Patterson, V. M.; Innis, R. B.; Pike, V. W. *J. Med. Chem.* **2007**, *50*, 3256.
21. Wang, J.-Q.; Tueckmantel, W.; Zhu, A.; Pellegrino, D.; Brownell, A.-L. *Synapse* **2007**, *61*, 951.
22. Tamagnan, G. D.; Batis, A. O. K.; Lee, H.; Alagille, D.; Jennings, D.; Russell, D.; Carson, R.; Marek, K.; Seibyl, J. P. *Eur. J. Nucl. Med. Mol. I.* **2009**.
23. Brown, A. K.; Kimura, Y.; Zoghbi, S. S.; Simeon, F. G.; Liow, J.-S.; Kreisl, W. C.; Taku, A.; Fujita, M.; Pike, V. W.; Innis, R. B. *J. Nucl. Med.* **2008**, *49*, 2042.
24. Lucatelli, C.; Honer, M.; Salazar, J.-F.; Ross, T. L.; Schubiger, P. A.; Ametamey, S. M. *Nucl. Med. Biol.* **2009**, *36*, 613.

25. Honer, M.; Stoffel, A.; Kessler, L. J.; Schubiger, P. A.; Ametamey, S. M. *Nucl. Med. Biol.* **2007**, *34*, 973.
26. Baumann, C. A.; Mu, L.; Johannsen, S.; Honer, M.; Schubiger, P. A.; Ametamey, S. M. *J. Med. Chem.* **2010**, *53*, 4009.
27. Wilson, A. A.; Jin, L.; Garcia, A.; DaSilva, J. N.; Houle, S. *Appl. Radiat. Isot.* **2001**, *54*, 203.
28. Jacobs, A. H.; Li, H.; Winkeler, A.; Hilker, R.; Knoess, C.; Ruger, A.; Galldiks, N.; Schaller, B.; Sobesky, J.; Kracht, L.; Monfared, P.; Klein, M.; Vollmar, S.; Bauer, B.; Wagner, R.; Graf, R.; Wienhard, K.; Herholz, K.; Heiss, W. D. *Eur. J. Nucl. Med. Mol. I.* **2003**, *30*, 1051.
29. Lee, C.-M.; Farde, L. *Trends Pharmacol. Sci.* **2006**, *27*, 310.
30. Shetty, H. U.; Zoghbi, S. S.; Simeon, F. G.; Liow, J.-S.; Brown, A. K.; Kannan, P.; Innis, R. B.; Pike, V. W. J. *Pharmacol. Exp. Ther.* **2008**, *327*, 727.
31. Pike, V. W. *Trends Pharmacol. Sci.* **2009**, *30*, 431.
32. Tipre, D. N.; Zoghbi, S. S.; Liow, J. S.; Green, M. V.; Seidel, J.; Ichise, M.; Innis, R. B.; Pike, V. W. *J. Nucl. Med.* **2006**, *47*, 345.
33. Wilson, A. A.; Houle, S. *J. Labelled Compd. Rad.* **1999**, *42*, 1277.
34. Ametamey, S. M.; Kessler, L. J.; Honer, M.; Wyss, M. T.; Buck, A.; Hintermann, S.; Auberson, Y. P.; Gasparini, F.; Schubiger, P. A. *J. Nucl. Med.* **2006**, *47*, 698.
35. Schinkel, A. H.; Wagenaar, E.; Mol, C. A. A. M.; vanDeemter, L. *J. Clin. Invest.* **1996**, *97*, 2517.
36. Wheeler, J. B.; Stourman, N. V.; Armstrong, R. N.; Guengerich, F. P. *Chemical Research in Toxicology* **2001**, *14*, 1107.
37. Bogaards, J. J. P.; Venekamp, J. C.; Salmon, F. G. C.; van Bladeren, P. J. *Chem. Biol. Interact.* **1999**, *117*, 1.
38. Bradford, M. M. *Anal. Biochem.* **1976**, *72*, 248.
39. Wang, Y.; Seidel, J.; Tsui, B. M. W.; Vaquero, J. J.; Pomper, M. G. *J. Nucl. Med.* **2006**, *47*, 1891.
40. Honer, M.; Bruhlmeier, M.; Missimer, J.; Schubiger, A. P.; Ametamey, S. M. *J. Nucl. Med.* **2004**, *45*, 464.
41. Mikolajczyk, K.; Szabatin, M.; Rudnicki, P.; Grodzki, M.; Burger, C. *Med. Inform.* **1998**, *23*, 207.